MEMORANDUM
RM-3251-PR
MAY 1963

406 204

RADAR ECHO FROM RE-ENTRY VEHICLES

Herschel Weil

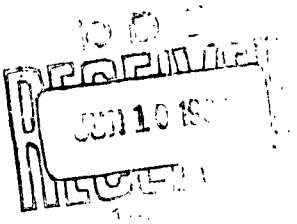

PREPARED FOR:
UNITED STATES AIR FORCE PROJECT RAND

The RAND Corporation
SANTA MONICA • CALIFORNIA

MEMORANDUM

RM-3251-PR

MAY 1963

RADAR ECHO FROM RE-ENTRY VEHICLES

Herschel Weil

This research is sponsored by the United States Air Force under Project RAND—contract No. AF 49(638)-700 monitored by the Directorate of Development Planning, Deputy Chief of Staff, Research and Development, Hq USAF. Views or conclusions contained in this Memorandum should not be interpreted as representing the official opinion or policy of the United States Air Force.

The RAND Corporation

1700 MAIN ST • SANTA MONICA • CALIFORNIA

PREFACE

This Memorandum discusses the results of a study to determine the nature of the radar return from laminar wakes. It is intended to supplement the knowledge of high-altitude re-entry phenomenology. The author is a consultant for The RAND Corporation. The results presented herein should be of general interest to those in the field of aerodynamics and electromagnetic theory.

SUMMARY

This Memorandum outlines the main aspects of the problem of computing the radar echo from re-entry vehicles, primarily to indicate what types of radar-return estimates can be made using presently available results from the gasdynamic theory of wakes and from electromagnetic theory. Numerical results for low-frequency reflectivities and radar cross sections are obtained for a particular computed re-entry wake viewed broadside. The resulting radar cross sections, although orders of magnitude greater than the radar cross section of the vehicle with no wake, are smaller than the broadside geometric cross section of the wake region within which the local plasma frequency is greater than the radar frequency. Some specific electromagnetic problems are outlined, the solution of which would aid in obtaining results better than the crude estimates presently achievable.

ACKNOWLEDGMENTS

The author would like to acknowledge the helpful discussions he has held in the course of this work with Mary Romig of The RAND Corporation and Paul Lykoudis of Purdue University on the flow problems, and with T.B.A. Senior of the University of Michigan on electromagnetics.

CONTENTS

SYMBOLS

$\bar{B}$ = magnetic field strength

C = cosine of angle between the incident propagation direction and the negative z-axis

c = velocity of light in a vacuum

E^m = incident electric field strength

E^s = scattered electric field strength

$\bar{E}$ = electric field

e = electronic charge

G = antenna gain

H = enthalpy

$\bar{H}$ = magnetic field intensity

$\vec{J}_m$ = effective magnetization current

k_μ = phase constant

k_χ = attenuation coefficient

M = Mach number

$\bar{M}$ = associated magnetization

m = mass

m_e = electron mass

N_e = number density of electrons

n = index of refraction

P = amplitude reflection factor

P_r = net power received

P_t = transmitted power

p = pressure, in atmospheres

R = Howarth radial distance

R_o = perpendicular range from the radar to the trail

r_o = body radius

S = function given by Eq. (21)

T = fluid temperature

U = velocity

v = particle velocity: integration volume where $n \sim 1$

x = axial distance increasing down the wake

α = polytropic coefficient

$\Gamma(x+1)$ = gamma function

γ' = effective ratio of specific heats

ϵ_o = free-space permittivity

ν = collision frequencies of electrons

ρ = density: distance from the scatterer

ω = 2π times radar operating frequency: radian frequency

ω_p = radian plasma frequency, proportional to $\sqrt{N_e}$

γ = curve fitting parameter

σ = radar cross section

C_D = drag coefficient

Subscripts

m = reference condition in an isentropic process

s = stagnation value

∞ = unperturbed value except when used with x; x_∞ is the minimum value at which the pressure in the wake can be taken as $p = p_\infty$

I. INTRODUCTION

The wakes we are concerned with are mixtures of neutral molecules and atoms, ions, and electrons. When an electromagnetic (e.g., radar) wave is incident, the electric field, $\bar{E}$, and magnetic field, $\bar{B}$, exert forces on the electrons and ions. At all radar frequencies the inertia of the ions is such that they are not appreciably accelerated, but the much lighter electrons respond to the field. They are accelerated and reradiate to cause the radar return or echo. In computing this effect, only the $\bar{E}$ field need be considered because the force exerted on a charged particle by the $\bar{B}$ field associated with $\bar{E}$ through Maxwell's equations is a factor v/c less than the force exerted by the $\bar{E}$ field, where v is the particle velocity, and c is the velocity of light in vacuo. Furthermore, at radar frequencies the effects of the earth's magnetic field can generally be neglected.

For any point along a vehicle's re-entry trajectory, the problem of computing the magnitude of the reradiation for a given incident electromagnetic field requires two quite different lines of research. The first line determines the number densities of the electrons, N_e, and their collision frequencies, ν, for momentum transfer to neutrals as functions of position in the wake. The second line, using the data generated by the first, determines the reradiation and hence reflectivity and radar return. With the present state of knowledge, only rough estimates or bounds on N_e and ν are available. Nevertheless, the electromagnetic theory is no better off, for only rough estimates of radar return are possible for those distributions of N_e and ν associated with the wake. Approximate methods must be used, and to determine what approximate approaches to use, some idea of the spatial variation of ν/ω and of ω_p/ω is needed. Here ω_p is the radian plasma frequency which is proportional to $\sqrt{N_e}$, while ω is 2π times the operating frequency of the radar. In Section II, methods for computing the necessary approximate distribution of N_e and ν are outlined and numerical results given. In Section III, the various approaches to the electromagnetic problems of determining radar cross section are discussed. The results

of Sections II and III are combined to yield reflectivities and radar cross sections in Section IV. Section V consists of a discussion of the electromagnetic problems which should be solved in order to obtain a more complete picture of the interaction between the radar and the wake.

II. ELECTRON AND COLLISION FREQUENCY DISTRIBUTIONS

We will consider, in this section, the distribution of electron density and collision frequency in the laminar wake behind blunt, non-ablating bodies. The wake will be taken to be in thermodynamic equilibrium. This model corresponds to that used by Feldman[1] and Lykoudis[2] and presents several restrictions on the flight regime which render the numerical examples calculated in this section somewhat unrealistic. The techniques, however, may be extended to other, more realistic cases by modification of the gas dynamic model.

The criterion of thermodynamic equilibrium is necessary in order to calculate the electron density with any sense of confidence. This will occur, for a body of one ft nose radius, at about 100,000 ft altitude, where the recombination rates are sufficiently fast to keep the gas in equilibrium even though it is cooling rapidly by its expansion around the body and in the wake. Above this altitude, say at 200,000 ft, the flow is frozen, and the ionization level is close to that at the stagnation region.

Turbulence, which would generally lower the electron density by increasing the cooling rates, is not considered here, although the altitude regime chosen for the numerical example is more likely to produce a turbulent wake than a laminar wake. An additional possible effect of turbulence on the electromagnetic problem is discussed in Section V. Ablation products, which in many cases will be abundant, are also not considered. Although the electromagnetic problem for a wake containing ablation products would be treated in the same way, the values of N_e occurring can be quite different. The flow problem in this case is more complicated, since the effects of the boundary layer could not be neglected as they otherwise can be.

For the equilibrium case, electron densities in the wake have been calculated by Feldman.[1] For this Memorandum an attempt was made to use the work of Lykoudis,[2] which contains an analytic expression for trail enthalpy, to develop a primarily analytic (and hence general) method of determining the electron density in the region

where trail cooling is primarily by conduction. In the end, however, it was found necessary to resort to a numerical approach pretty much like Feldman's, but with some simplification, most of which is due to using Lykoudis' results. The present numerical results, are in close agreement with those of Feldman (to the extent that they can be scaled off his published curves of constant N_e contours).

The electron density is a function of the thermodynamic variables ρ and T, where ρ is the density and T is the fluid temperature. The collision frequency, on the other hand, is most conveniently expressed as a function of p and T, where p is the pressure. A suitable equation of state for high-temperature air may be used to relate p, ρ, and T. The pressure and temperature in the wake are obtained from the various gas-dynamic calculations mentioned previously.[1,2]

Shkarofsky[3] has correlated extensive experimental data on the collision frequency which show that in the temperature range of approximately $1800^{\circ}K < T < 3400^{\circ}K$, ν/p can be taken as a constant; i.e.,

$$\nu \sim p \times 7 \times 10^{10} \tag{1}$$

where p is in atmospheres. The pressure along the axis may be approximated by use of Sakurai's second-order blast-wave theory as given, for example, by Lykoudis[2] in terms of the free-stream Mach number, M_∞, and the body radius, r_o

$$\frac{p}{p_\infty} = 0.1330 \frac{M_\infty^2}{x/r_o} + 0.405 \tag{2}$$

Here x is measured from the stagnation region, and the formula is valid from the nose at $x = x_s$ to the axial position $x = x_\infty \simeq M_\infty^2 r_o/4.5$ where p has decayed to the free-stream pressure, p_∞. For greater values of x, p remains equal to p_∞, there is no flow expansion, and trail cooling is due to heat conduction alone. The accuracy of Sakurai's theory has been exhibited by Feldman,[4] who compared numerical axial-pressure results with results computed by exact theory using the method of characteristics.

Values of electron density for air in equilibrium may be obtained from Gilmore's tables and graphs[5] or from Feldman.[1] In the range $2500^{\circ}K < T < 7000^{\circ}K$, the numerical results for N_e can be fitted within a factor of approximately two by

$$N_e = \left(\frac{\rho}{\rho_o}\right)^{0.7} 10^{(T \times 10^{-3} + 15)}, \qquad m^{-3} \tag{3}$$

where T is in $^{\circ}K$, and $\rho_o = 1.29$ kg/m^3 is the density at $273^{\circ}K$ and 1 atm pressure.

In order to evaluate Eq. (3), a relationship between T and x must be obtained. For the expansion region of the trail, $x_s < x < x_\infty$, cooling takes place adiabatically by a purely isentropic, or constant-entropy, process. For air, Logan and Treanor[6] have calculated the polytropic coefficients γ' and α for an isentropic process as functions of entropy which relate the state variables p, ρ, T, and the enthalpy, H, through the following equations*

$$\frac{T}{T_m} = \left(\frac{p}{p_m}\right)^{\frac{\gamma'-1}{\gamma'}} = \left(\frac{\rho}{\rho_m}\right)^{\gamma'-1}$$

$$\frac{T}{T_m} = \left(\frac{H}{H_m}\right)^{\alpha} \tag{4}$$

As a practical matter, since it is necessary to compute the entropy or read it from shock tables in order to obtain the proper values for γ' and α, there is no simple, purely analytic way to determine the variables from the free-stream pressure even with the help of the blast-wave equation for pressure. For specific numerical results it is probably just as easy to use a Mollier diagram as it is to use the above equations.

*Logan and Treanor write Eq. (4) with different constants γ' and γ'' for the p and ρ terms, but give almost identical numerical values for them.

Since the wake will be expanding in a radial as well as an axial direction, the temperature, and hence the electron density, will vary in that direction as well. It appears[4] that the various approximate theories give only very poor results for flow parameters off the axis for regions very close to the shoulder. However, numerical values obtained by the method of characteristics are given by Feldman in Ref. 1.

Lykoudis[2] developed the following equation for the enthalpy at $x = x_\infty$ in terms of the Howarth radial distance R from the axis

$$\frac{H(x_\infty, r) - H_\infty}{H(x_\infty, 0) - H_\infty} = \frac{1}{\left(1 + \frac{4fR^2}{2.56\, C_D r_o^2}\right)^{0.847}} \tag{5}$$

and compared it with a Gaussian approximation

$$\frac{H(x_\infty, r) - H_\infty}{H(x_\infty, 0) - H_\infty} \sim \exp\left[\frac{-R^2}{C_D r_o^2}\right] \tag{6}$$

used by Feldman in Ref. 1, which drops off a little faster with r. In these equations, H_∞ is the enthalpy in the undisturbed atmosphere at the altitude in question. The Howarth radius, R, is related to the physical radius, r, by

$$r^2 = 2 \int_0^r [\rho_\infty/\rho\,(R)]\, R\, dR$$

For $x > x_\infty$ the axial enthalpy distribution is given in a universal form by Lykoudis as

$$\frac{H(\bar{x}, 0) - H_\infty}{H(0, 0) - H_\infty} = \frac{1}{(1 + \bar{x})^{0.8}} \tag{7}$$

where

$$\bar{x} = \frac{[H(0, 0)/RT_o]^{\frac{1}{4}}}{415\, \rho_\infty U_\infty} \frac{x - x_\infty}{C_D r_o^2}$$

and centimeter-gram-second units are to be used.

With the radial enthalpy distribution at the point $x = x_\infty$ given by Eq. (5), the radial enthalpy distribution at any x could be obtained from Eq. (7). However, if the less accurate Gaussian form, Eq. (6), is used, the corresponding enthalpy ratio for $x > x_\infty$ must have the form

$$\frac{H(x, r) - H_\infty}{H(x_\infty, 0) - H_\infty} = \frac{1}{\Sigma^2(\bar{x})} \exp\left[\frac{-R^2}{\Sigma^2(\bar{x})\, r_o^2}\right] \tag{8}$$

Then $\Sigma^2(\bar{x})$ will be chosen to make Eq. (8) match Eq. (7) on the axis.

In the range $x > x_\infty$ Eqs. (2) and (4) do not hold, and the only reasonable way to get T and ρ and thence N_e is to follow the log p_∞/p_o = const. curve on the Mollier chart using Eq. (7) for the enthalpy. This has already been done along the axis in Ref. 2.

To get the radial electron density we equate

$$\frac{1}{\Sigma^2(\bar{x})} = \frac{1}{(1 + \bar{x})^{0.8}} \tag{9}$$

and use this in Eq. (8) to find the values of enthalpy to enter the Mollier diagram. Eqs. (8) and (9) agree with Eq. (6) for $C_D \sim 1$.

The outline of the computational procedure just presented makes it clear that analytic formulas directly yielding the electron-density contours are not available from present flow computations. One must compute the density contours, and then perhaps reasonable empirical formulas can be fitted.

Numerical results for an altitude of 100,000 ft and a velocity U_∞ = 20,000 ft/sec follow. Reference 7 shows that the unperturbed

values (subscript ∞) and stagnation values (subscript s) are*

$$p_\infty = 1.102 \times 10^{-2} \text{ atm} \qquad p_s = 6.33 \text{ atm}$$

$$\rho_\infty = 1.385 \times 10^{-2} \rho_o \qquad \rho_s = 0.183\ \rho_o$$

$$T_\infty = 218^\circ K \qquad T_s = 6930^\circ K$$

$$\frac{H_\infty}{RT_o} = 2.783 \qquad \frac{H_s}{RT_o} = 239$$

The shock tables yield an entropy S = 2.86 cal/gm-$^\circ$K. With this value one can enter Logan and Treanor's graphs for the polytropic coefficients and find that $\gamma' = 1.13$, and $\alpha = 0.7$. At $x = x_\infty$, $p = p_\infty$, and from Eq. (4), $T = 3300^\circ K$. The Mollier diagram yields about $3200^\circ K$, which is certainly sufficiently consistent. The value of ρ corresponding to a temperature of $3300^\circ K$ is given by $\log [\rho\ (x_\infty)/\rho_o] = -3.05$ for which the graphs of Ref. 2 yield $N_e = 2.4 \times 10^{16}/m^3$ while, for comparison, the approximate formula Eq. (3) yields $N_e = 4.8 \times 10^{16}/m^3$.

This is the electron number density on the axis where $p = p_\infty$, which occurs at $x_\infty = 93.1\ r_o$, since $M_\infty = 20.5$. The normalized enthalpy $H\ (x_\infty,0)/RT_o = 86$ so that $\bar{x}$, the normalized distance used in Eqs. (7) and (8) for the enthalpy variation, is given by

$$\bar{x} = 6.7 \times 10^{-2} \frac{x - x_\infty}{C_D r_o^2} \qquad (10)$$

where lengths are to be expressed in centimeters.

To delimit the region in which values of N_e should be computed let us assume that the main radar return is from the region in which, as will be discussed in Section III, $\omega\nu \lesssim \omega_p^2$. The collision frequency $\nu(x_\infty,0) = 7.9 \times 10^8$ cps for $p_\infty = 1.1 \times 10^{-2}$ and ν will remain essentially

*Note that with the present notation, $p_\infty = p(x_\infty)$, but $H_\infty \neq H(x_\infty)$, $\rho_\infty \neq p(x_\infty)$, etc.

constant until the trail cools to $T \tilde{\sim} 1800^{\circ}K$. For various reasons* one would expect that the lowest frequency which will be used by the radar will be of the order of $f \sim 10^8$ cps. On this assumption a lower bound for N_e values of interest would correspond to $\omega_p \sim 10^8$ or $N_e \sim 3 \times 10^6/cm^3$.

Figure 1 presents a family of curves of N_e versus r/r_o with $\bar{x}$ as parameter, for an altitude of 100,000 feet and a velocity of 20,000 ft/sec. From this data a set of curves of $N_e/N_{e_{max}}$ verus r/r_o were computed. These are shown in Figure 2. On each curve is superposed one or two curves of $S = \text{sech}^2 \left(\frac{1}{2\tilde{\sigma}} \frac{r}{r_o}\right)$ for values of $\tilde{\sigma}$ as indicated on the curves. These will be used to aid in estimating radar return (see Section III, pp. 17, 18).

*One reason is that, if f is lower than $\sim 2 \times 10^7$ cps the radar will be unable to penetrate the F layer of the ionosphere even at vertical incidence to acquire and track objects above the ionosphere.

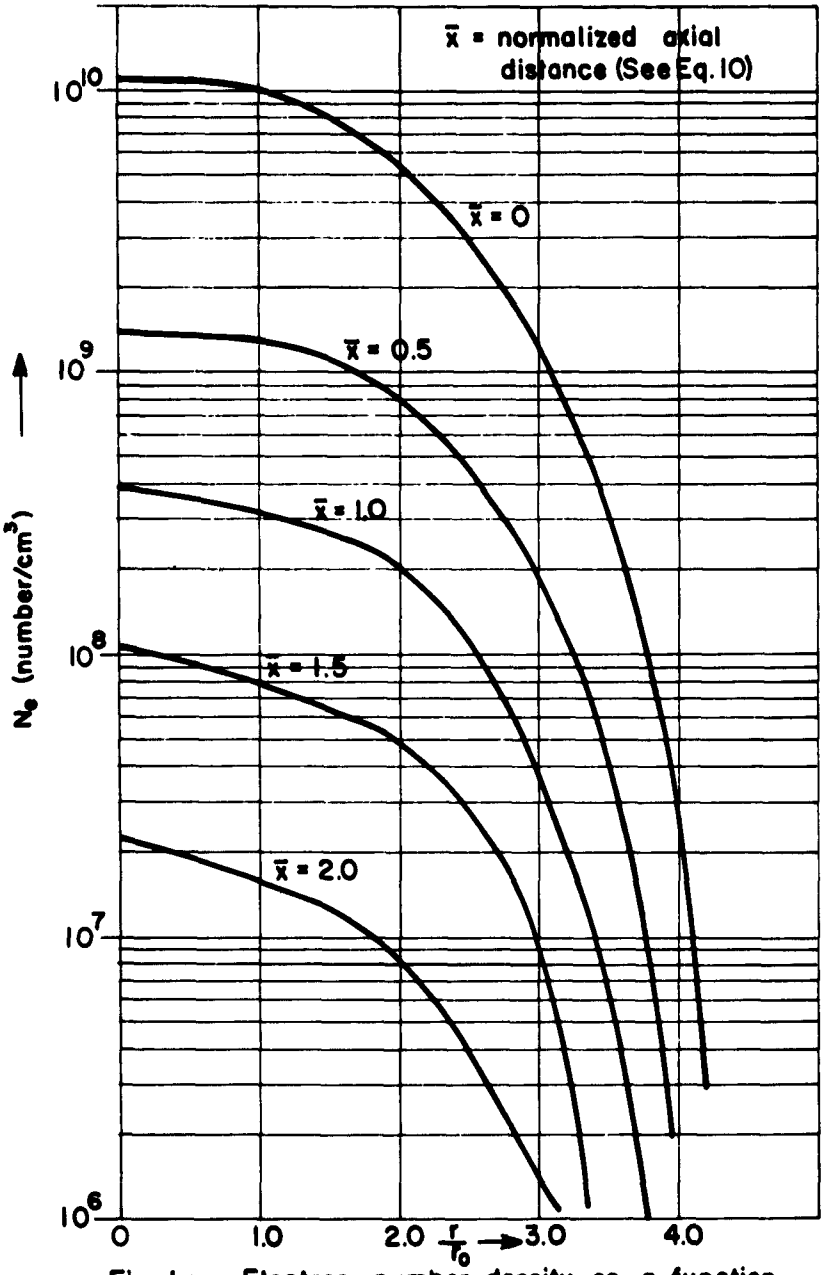

Fig. 1 — Electron number density as a function of radial distance from axis.

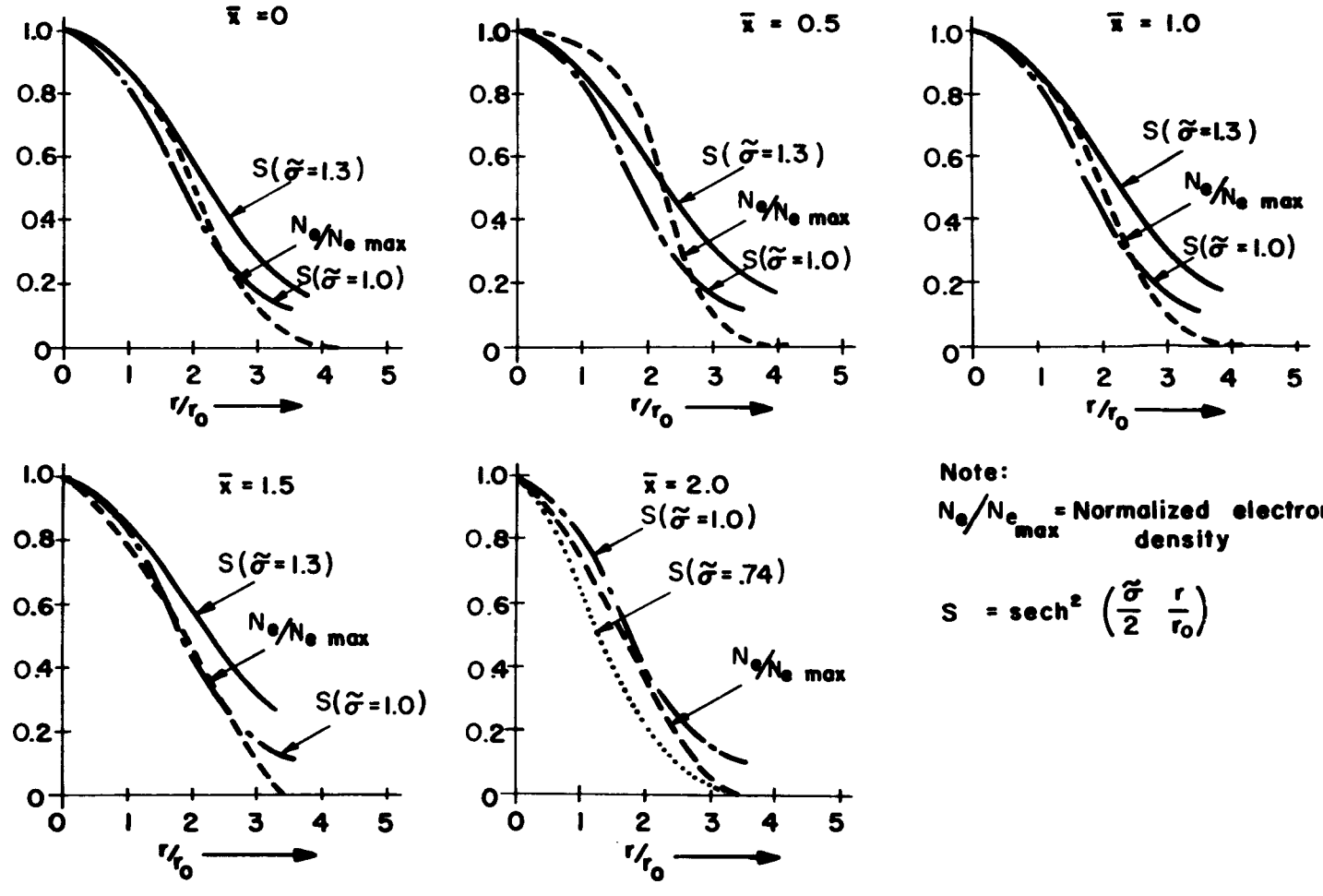

Note:

$N_e/N_{e\ max}$ = Normalized electron density

$S = \text{sech}^2\left(\frac{\tilde{\sigma}}{2}\ \frac{r}{r_0}\right)$

Fig. 2 — Normalized electron number density and sech^2 curves

III. REFLECTIVITY AND RADAR RETURN

The radar beam and its echo are electromagnetic waves: that is, they are composed of fields of electric intensity, $\overline{E}$, and magnetic induction, $\overline{B}$, which are related by Maxwell's equations. These equations are most conveniently written for the present problem as

$$\begin{aligned} \text{curl } \overline{E} &= -\frac{\partial \overline{B}}{\partial t} \\ \text{curl } \overline{B} &= \frac{n^2}{c^2}\frac{\partial \overline{E}}{\partial t} \end{aligned} \tag{11}$$

Here c is the velocity of light in free space and n is the index of refraction. We shall consider time-periodic fields of radian frequency ω so that time variation can be separated out in a factor $e^{-i\omega t}$. At each point the index of refraction is a function of ω, ω_p, and ν. It is determined by considering Eq. (11) coupled with the equations for conservation of number of electrons and ions, and of conservation of momentum. By not having n^2 operated on by $\partial/\partial t$, we are tacitly assuming that time variations of n^2 are negligible over a period of the order of the time a radar pulse spends in the wake. In addition, Eq. (11) assumes the medium is homogeneous and isotropic and that the permeability is constant everywhere. To the writer's knowledge, there are no exact solutions of Eq. (11) for regions of continuously variable n except for certain one-dimensional problems. Hence for results at this time, approximate methods will have to be used.

Much of the directly applicable theory has been developed by workers in ionospheric radio propagation, so that the notation frequently used in that field will be adopted here.* The index of refraction is a complex quantity when $e^{-i\omega t}$ time-dependence is used and is written as

$$n = \mu + i\chi \tag{12}$$

*The notation and much of the material in this section up to Eq. (22) plus the supporting analyses are conveniently found in a monograph by Budden.(8)

A plane electromagnetic wave propagating in the z direction through a uniform medium of index n is a solution of Eq. (11) which has the form

$$\bar{E}(z,t) = \bar{E}_o e^{ik\mu z} e^{-k\chi z} e^{-i\omega t} \qquad (13)$$

and for which $\bar{E}_o \cdot \hat{z} = 0$; that is, vector $\bar{E}_o$ is perpendicular to the unit vector $\hat{z}$ in the z direction. In Eq. (13), $k = \omega/c = 2\pi/\lambda_o$ is the free-space wavelength. By means of Eq. (13) a physical interpretation of n is made evident; $k\mu$ represents a phase constant and $k\chi$, an attenuation coefficient for plane waves in a uniform medium. In free space, $\chi = 0$ and $\mu = 1$.

If the electric field expressed by Eq. (13) is connected with electromagnetic field $\bar{H}$ so that it contributes to electromagnetic radiation via Poynting's vector $\bar{E} \times \bar{H}$, then $\bar{E}_o \cdot \hat{z} = 0$. However, in plasmas, additional $\bar{E}$ fields of the form of Eq. (13) can exist, but for which $\bar{E}_o \cdot \hat{z} \neq 0$. These so-called longitudinal or plasma modes can greatly affect the distribution of energy within the plasma; although far from their sources, they are not paired with a magnetic field so as to radiate electromagnetic energy (zero Poynting vector). It is necessary to determine whether such modes can be expected in the wake plasma. If so, they would certainly influence the reradiation pattern since incident electromagnetic energy can be transferred to and from such modes by various mechanisms that have been the subject of much study in the literature. Whether these longitudinal modes can exist or propagate at the frequencies of interest is a function of the physical properties of the plasma which, for this wake problem, were determined numerically for the wake in Section II. These properties can then be used to evaluate criteria formulated by Denisse and Delcroix[9] for the existence of the various propagation modes in a plasma, which indicate that one would not expect such modes. In fact, one is in a region where only transverse electromagnetic propagation is to be expected. Moreover, since magnetic-field effects may also be neglected, barring possible effects of turbulence, the index of refraction, n, for these electromagnetic waves is quite simple in form.

The electron number density, N_e, enters the expression for n only in combination with the electron charge, e; mass, m; and the free-space permittivity, ϵ_o; to form a frequency

$$\omega_p = \sqrt{\frac{N_e e^2}{m \epsilon_o}} \tag{14}$$

which one can show is a natural frequency for coherent oscillation of the plasma. It is convenient to work with variables normalized by the radian frequency, ω

$$X = \frac{\omega_p^2}{\omega^2}, \quad Z = \frac{\nu}{\omega} \tag{15}$$

Then

$$n^2 = 1 - \frac{X}{1 + iZ} \tag{16}$$

Let $n^2 = \epsilon_r + i\epsilon_i$, where n^2 is commonly called the complex dielectic constant. Then

$$\begin{aligned} \epsilon_r &= 1 - \frac{X}{1 + Z^2} \\ \epsilon_i &= \frac{ZX}{1 + Z^2} \end{aligned} \tag{17}$$

and μ and χ may be computed from

$$\begin{aligned} \mu &= \frac{1}{\sqrt{2}} \left(\epsilon_r + \sqrt{\epsilon_r^2 + \epsilon_i^2} \right)^{1/2} \\ \chi &= \frac{1}{\sqrt{2}} \left(-\epsilon_r + \sqrt{\epsilon_r^2 + \epsilon_i^2} \right)^{1/2} \end{aligned} \tag{18}$$

From Eqs. (17) and (18) we can get a feel for the situation in which μ and χ differ appreciably from the ambient values. We have $\epsilon_r \sim 1$, and $\epsilon_i \sim 0$ so that $\mu \sim 1$ and $\chi \sim 0$ (the values for a vacuum) whenever

$$Z^2 \gg X, \text{ i.e., } \nu^2 \gg \omega_p^2$$

On the other hand, ϵ_r and ϵ_i can differ appreciably from $\epsilon_r \sim 1$ and $\epsilon_i \sim 0$ when

$$Z \sim X, \text{ i.e., } \omega\nu \sim \omega_p^2$$

or when

$$Z < X, \text{ i.e., } \omega\nu < \omega_p^2$$

The equality $\omega\nu = \omega_p^2$ defines a situation in which ν may exceed ω_p so long as ω is less than ω_p; i.e., $\omega < \omega_p < \nu$.

The commonly used idea of perfect reflectivity at a constant N_e surface corresponding to $\omega = \omega_p$ stems from the formula for the amplitude reflection factor, P, for normal incidence of a plane wave onto a plane interface separating homogeneous media of refractive indices n_1 and n_2

$$P = \frac{n_2 - n_1}{n_2 + n_1} \tag{19}$$

Let $n_1 = 1$, corresponding to free space for medium 1. If collisions are neglected, $Z \ll 1$ and $n_2^2 = 1 - X$. Then if $X \gg 1$, n_2 is purely imaginary and $|P| = 1$, indicating complete reflection of the energy.

It is important in the present wake problem to observe that this conclusion is much modified when Z is not negligible compared to unity. In this case, the surface $\epsilon_r = 0$ corresponds to $\epsilon_i = Z$ and $\mu = \chi = \sqrt{Z/2}$. For simplicity, let $n_1 = 1$ again in Eq. (19) for P; then

$$|P|^2_{\epsilon_r = 0} = \left. \frac{(\mu - 1)^2 + \mu^2}{(\mu + 1)^2 + \mu^2} \right|_{\mu = Z/2} < 1$$

Table 1, which presents $|P|^2_{\epsilon_r = 0}$ versus Z, illustrates that from the point of view of reflectivity, surfaces corresponding to constant plasma frequencies are of little significance when the collision frequency is within a factor of about 100 from the operating frequency. Note, however, that a sharp boundary with unity index on one side is not a realistic model for plasmas. For large Z there would be, in a more realistic case of no sharp boundary, very great absorption of the energy before the surface $\epsilon_r = 0$ is reached.

Table 1

Z	$\lvert P\rvert^2_{\epsilon_r = 0}$	Z	$\lvert P\rvert^2_{\epsilon_r = 0}$
0.0002	0.96	2.0	0.20
0.005	0.82	8.0	0.40
0.02	0.67	200.0	0.82
0.08	0.465	450.0	0.89
1.0	0.17	800.0	0.91

The reflectivity considerations are also much modified by the fact that, in a plasma, there are no such discontinuities as those that led to Eq. (19). In fact, the reflectivity is a functional of the gradient of N_e in the direction of propagation. As will be shown below, however, even in the one-dimensional case, where N_e varies with X at a constant Z, it is a considerable mathematical problem to determine the reflectivity and the related transmissivity. In general, asymptotic procedures must be used to pick out and relate appropriate solutions of the electromagnetic-field equations. In particular, solutions have been obtained for a wide class of these curves known as Epstein profiles plus generalizations of them by Rawer.[10] Included in this class of profiles are the so-called sech^2 profiles

$$n^2 = 1 - \frac{X_m}{1 - iZ} \operatorname{sech}^2 \left\{ \frac{1}{2\tilde{\sigma}} (z - z_m) \right\} \tag{20}$$

so that

$$X = X_m S(z - z_m; \tilde{\sigma}); \quad S = \operatorname{sech}^2 \left\{ \frac{1}{2\tilde{\sigma}} (z - z_m) \right\} \tag{21}$$

Here $\tilde{\sigma}$ is an arbitrary parameter.

This is a profile, symmetric about $z = z_m$, and representing a plasma layer. The reflection factor for normal incidence and $\overline{E}$ parallel to surfaces of constant electron density is given by

$$P = - \frac{\Gamma(-2ik\tilde{\sigma}C + 1)}{\Gamma(2ik\mu C + 1)} \frac{\Gamma(2ik\tilde{\sigma}C - \gamma - \frac{1}{2})}{\Gamma(-\gamma + \frac{1}{2})} \frac{\Gamma(2ik\tilde{\sigma}C + \gamma + \frac{1}{2})}{\Gamma(\gamma + \frac{1}{2})} \tag{22}$$

where

$$- \frac{16 k^2 \tilde{\sigma}^2 X_m}{1 - iZ} + \frac{1}{4} = \gamma^2$$

$\Gamma(x + 1)$ is the gamma function, and C is the cosine of the angle between the incident propagation direction and the negative z-axis. This complicated formula has been extensively investigated numerically by Rawer, who gave curves of $|P|$ versus ω/ω_1 for various values of ν/ω_1 and S_1, where $\omega_1 = \omega_p$ $(z = z_m)$ and $S_1 = 2\,\omega_1\tilde{\sigma}/c$. His results clearly illustrate the sensitivity of P to ν and to the gradients of N_e. Besides illustrating the sensitivity of reflectivity on the details of the plasma layer, the Rawer results could be used to give local reflectivity as a function of axial distance along the trail. The computations of the previous section yielded values of N_e and ν, which determine X as a function of r where r is the radial distance from the trail axis. One can equate r with $z - z_m$ of Eq. (20) and use the parameter $\tilde{\sigma}$ to fit the distribution of Eq. (21) for X to that of the computed X distribution.* Depending on the X and Z values, P may be obtained directly from Rawer's curves. If not, P can be readily computed from Eq. (22) with the help of tables of the complex gamma function.

Ionospheric problems are by no means the only ones where one-dimensional propagation in a medium of varying n has been investigated. It has been of interest to others for application to precisely the same type of problem as the present vehicle-wake investigation: for microwave diagnostics of plasmas in fusion machines, ballistic ranges, shock tubes, etc., and for the design of radar absorbers. For example, Albini and Jahn have computed numerically a large number of curves of reflectivity and transmissivity for various degrees of lossiness of the plasma as measured by ϵ_i and for ramp and trapezoidal variations of ϵ_r.[11,12] These curves cover regions where WKB analyses break down (as they will in all the trail problems of interest) so that the analytic treatment becomes difficult, as Ref. 11 illustrates; therefore, numerical methods are used. On the other hand, the distributions shown in these curves have discontinuous gradients that introduce reflection and interference phenomena which would not show up in a region where the gradient varies smoothly. The effect of discontinuous gradients and gradients that cause WKB asymptotic approximations to fail is discussed in various parts of Ref. 8 (see

*This process is illustrated in Fig. 2.

for example Section 17.4), and the fact that a discontinuity in the electron-density gradient actually changes the reflection coefficient by an order of magnitude is discussed by Schelkunoff.[13]

Much numerical and theoretical work has been done by Walther, who was interested in radar-absorber design. This work[14] was mainly concerned with varying dielectric-material parameters. Most of the analysis is based on the theoretical work of Barrar and Redheffer, described primarily in Ref. 15. Principles and techniques similar to those of Barrar and Redheffer have been tentatively applied to problems of this type by Bellman and Kalaba,[16] who introduced the term "method of invariant imbedding" for their work. The technique of invariant imbedding leads to various differential and integral equations which can be solved numerically, for example, to obtain the reflection factor as a function of penetration distance into a non-uniform medium.

At the Second Symposium on the Plasma Sheath, Boston, April 1962 (sponsored by AFCRC), C. M. DeRidder and S. Edelberg[17] reported the results of very extensive and instructive machine calculations of the reflectivity or backscattered energy per unit length for plane waves incident normally on an infinite plasma cylinder with uniform properties in the axial direction. Various analytic forms and numerical values were assumed for the index of refraction as a function of the radial distance from the axis. The $\overline{E}$ vector or $\overline{H}$ vector was taken parallel to the axis. The reason that this problem is especially adaptable to numerical solution is discussed in Section V, as are the difficulties of generalization.

How to use the reflectivities in determining radar return from the wake is a considerable problem, since the returns associated with much simpler problems involving either well-defined perfectly reflecting bodies or uniform dielectrics cannot really be handled at present except by approximate methods. Even the extensive numerical work of Ref. 17, for example, gives unrealistic results when applied to the wake problem, since the results show the power that would be received per unit length by an infinitely long antenna aligned with the infinite

cylinder. This type of difficulty and a partial solution is discussed by Brysk.[18] However, this difficulty is in a sense an artificial one, since in the physical problem the wake is finite.

What we shall do is realize that the wake is of a fairly restricted effective length when viewed near broadside and thereby avoid the difficulties in interpreting infinite-cylinder results. The numerical results in Section IV for reflectivity, $|P|$, show that for $\bar{x}$ up to some fairly well-defined value $\bar{x}_m$, the reflectivity does not vary greatly and that for $\bar{x} \gtrsim \bar{x}_m$ it drops rapidly to very small values. The trail for $x > \bar{x}_m$ will therefore be neglected, while up to $x = \bar{x}_m$ it will be considered to be cut into elementary segments $d\bar{x}$. These segments do not have well-defined ends of discontinuous electromagnetic properties which would be dominant scatterers; if they did, the discontinuities would combine to give pronounced resonant effects that would depend on the length. Such cylinders, if perfectly conducting, could be treated as so-called thick cylinders as is done in detail by Mentzer.[19] Their radar cross section is roughly

$$d\sigma_c = \frac{4\,(d\bar{x})^2}{\pi}\; s\,(ka) \tag{23}$$

for broadside incidence, where s(ka) oscillates in the shaded region of Fig. 3 about the line of 45-deg slope and converges asymptotically to this line. The upper bound is reached for $\bar{E}$ parallel to the symmetry axis; the lower bound occurs when H is parallel to the axis. Here k is the 2π/free-space wavelength and a is the cylinder radius.

Recalling the basic definition for radar cross section σ

$$\sigma = 4\pi \lim_{\rho \to \infty} \rho^2 \left| \frac{E^s}{E^m} \right|^2 \tag{24}$$

where ρ is distance from the scatterer, and where E^s and E^m are the scattered and incident field strengths, we see that the magnitude of the scattered field is then proportional to $\sqrt{\sigma}$. To account for the fact that we have, in fact, a nonperfect conductor so that

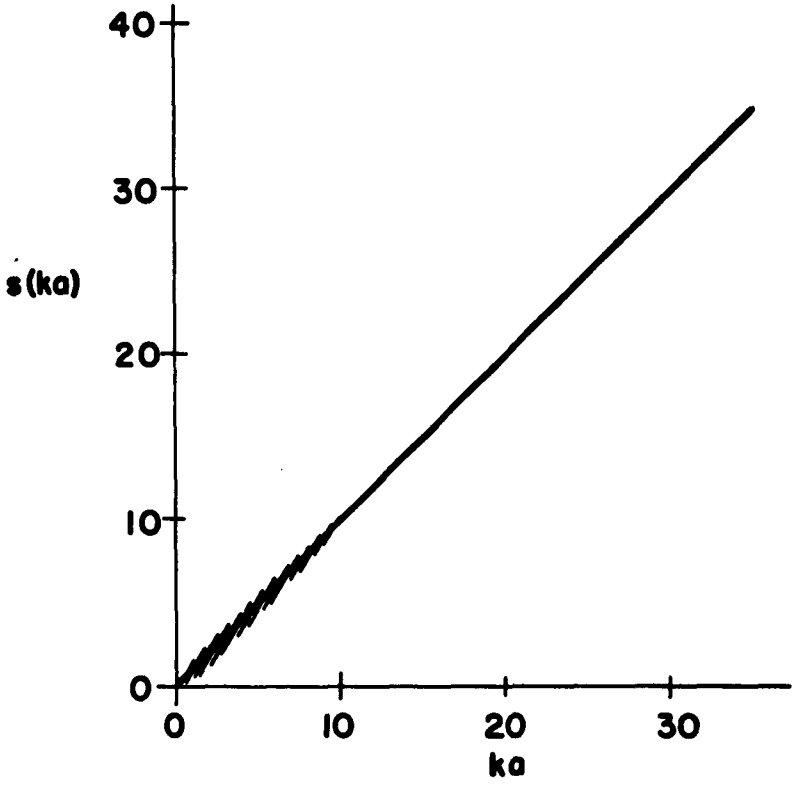

Fig. 3 — Cross-section factor, s(ka)

Eq. (23) cannot be used unmodified, we will do two things with only tenuous justification in order to get an effective scattered field.

We will first decide what to use for a. In those cases where the surface corresponding to the plasma frequency ($r = r_c$) is a very highly conducting surface, we could use $a = r_c$. To do this requires that operating frequencies corresponding to a range given roughly by $0.01 < \frac{\omega}{\nu} < 100$ be excluded, as shown by Table 1, since within this frequency range there is no reason to expect a critical-density contour to behave in any way like a perfect conductor.

When the plasma frequency is such that $a = r_c$ has not much physical significance, what is probably the next best choice is based on noting that the N_e versus r curve must have an inflection point at some value $r = r_i$. The major part of the reflectivity must come from the region $r < r_i$, since it is in this region that the steepest gradients of N_e exist. This suggests using $a = r_i$, which is done in Section IV. The second modification is to multiply $\sqrt{\sigma_c(kr_i)}$ by P to take into account the reflectivity. The justification for simply multiplying $\sqrt{\sigma_c}$ by P is that Refs. 20, 21, and 22 show by experiment, theory, and computation that the radar cross section for uniformly coated, perfectly conducting cylinders and spheres is approximately the radar cross section for the perfectly conducting object multipled by the power-reflection factor for a half space of the coating material. This approximation improves as ka increases, but it is good for ka not much greater than one if only order-of-magnitude results are wanted, which is the most we can hope for by this procedure.

The result of the above assumptions is to approximate the radar cross section of the trail section from $\bar{x} = 0$ to $\bar{x} = \bar{x}_m$ by

$$\sigma = \frac{4}{\pi} \left| \int \sqrt{s\,(kr_i)}\; |P|\; \exp\,[\arg P + k\Delta]\; d\bar{x} \right|^2 \qquad (25)$$

In addition to a phase of P, the phase $k\Delta$ due to variation in path length from the source to the integration points $\bar{x} > 0$ is included in this integral. If R_o is the perpendicular range from the radar to the trail when the region about $\bar{x} = 0$ is viewed broadside

$$\Delta \sim \frac{x^2}{2R}$$

The effect of antenna-gain pattern can be included in the factor $|P|$.

If the effective trail is long enough, the σ_c for off-broadside incidence should be used. This is available in Ref. 19. Similarly, P for off-broadside incidence ($C \neq 1$) should be used with a bistatic diffraction-pattern correction.

The contribution to returned power from regions in the wake where $P \sim 0$ will not be zero, although such echoes will be relatively small per unit length of trail compared to regions where Eq. (25) is usable. However, under some cases such regions may dominate the net return, for example, because the denser wake regions are not being irradiated.

In regions where $n^2 \sim 1$, refraction and phase retardation are negligible, and we can set up an integral for the radar return from the individual electrons. The backscattered energy reradiated by an individual electron per unit solid angle per unit incident power density is

$$\sigma_e = e^4 / (4\pi \epsilon_o m c^2)^2$$

Here e is the electron charge and m_e is the electron mass. The net power received, P_r, for transmitted power, P_t, is

$$P_r = \frac{\lambda^2 \sigma_e P_t}{16\pi^2} \left| \int_v \frac{G}{r^2} e^{-2ikr} N_e \, dv \right|^2 \qquad (26)$$

where G is the antenna gain and r is the distance to the scattering electron. Equation (26) is a volume integration rather than a line integral, since the contributions from each cross section have not been integrated in advance as they essentially were in Eq. (25) by the use of P (x). The integration volume, v, refers only to the region where $n \sim 1$. Equation (26) has been used to determine radar scattering from satellite wakes[23] and, in Ref. 24 and elsewhere, from low-density meteor trails. Contributions to the echo from other regions must be handled either approximately by Eq. (25) or by other means--for example, by a hybrid method introduced by Brysk[25] to handle scattering from overdense meteors.

IV. REFLECTIVITY AND RADAR CROSS-SECTION NUMERICAL RESULTS

The reflectivity factor P given by Eq. (22) was computed* as a function of $\bar{x}$ for two frequencies, $f = 2 \times 10^7$ and $f = 10^8$. The frequency $f = 2 \times 10^7$ is about the lowest that can be expected to penetrate the F layer of the ionosphere at normal incidence and hence is most likely a lower bound on frequencies which might be adopted for tracking re-entry objects. Figures 4 through 8 give $|P|$, $\ln|P|$, arg P, cos(arg P), and sin(arg P) for $f = 2 \times 10^7$ cps, while Fig. 9 through 13 do the same for $f = 10^8$ cps. In each case, there is a substantial trail region $\bar{x} < \bar{x}_m$ wherein $|P|$ does not vary by more than an order of magnitude. For larger $\bar{x}$ values it then very rapidly decreases to insignificance. However, even over the region where $|P|$ is not insignificant, the phase of Re(arg P) changes sign several times so that there is a tendency for the echoes from successive sections of the trail to be out of phase with each other and to partially cancel their respective contributions to the net return.

In addition to the above curves, we have also computed one value of P for $\bar{x} = 0$, $f = 10^{10}$. The result is $-\ln|P| = 1544$, arg $P = 15.8$.

To obtain some radar-cross-section values we have used Eq. (25), assuming Δ can be neglected because of the large range. From the inflection point of the curves in Fig. 2, a was taken to vary from $2.25\ r_o$ to $2.8\ r_o$ as $\bar{x}$ increased from $\bar{x} = 0$ to $\bar{x} = \bar{x}_m$. For this rough work we could simply take an average $a \sim 2.6\ r_o$ and hence factor s(ka) out of the integral. The integration was carried out in terms of the dimensionless variable $\bar{x}$ related to $x - x_o$ via Eq. (10). Further, the contribution of the region for $x < x_\infty$ was not included. The actual formula evaluated for σ was

$$\sigma = \frac{4}{\pi}\left(\frac{C_D\, r_o^2}{6.7 \times 10^{-2}}\right)^2 s(ka)\, |I|^2$$

*Numerical values of the complex Γ function were obtained from Ref. 26 or when outside the range covered in Ref. 26, by using asymptotic formulas.

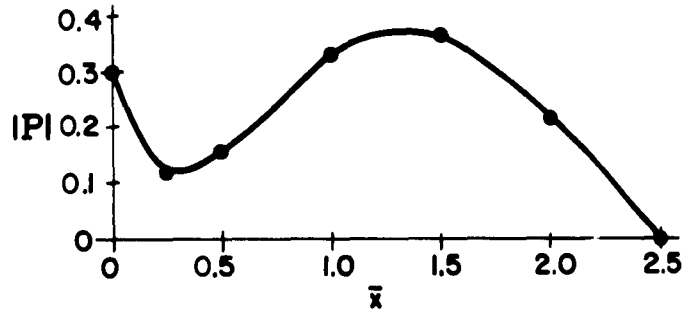

Fig. 4— Magnitude reflection factor, $|P|$ ($f = 2 \times 10^7$)

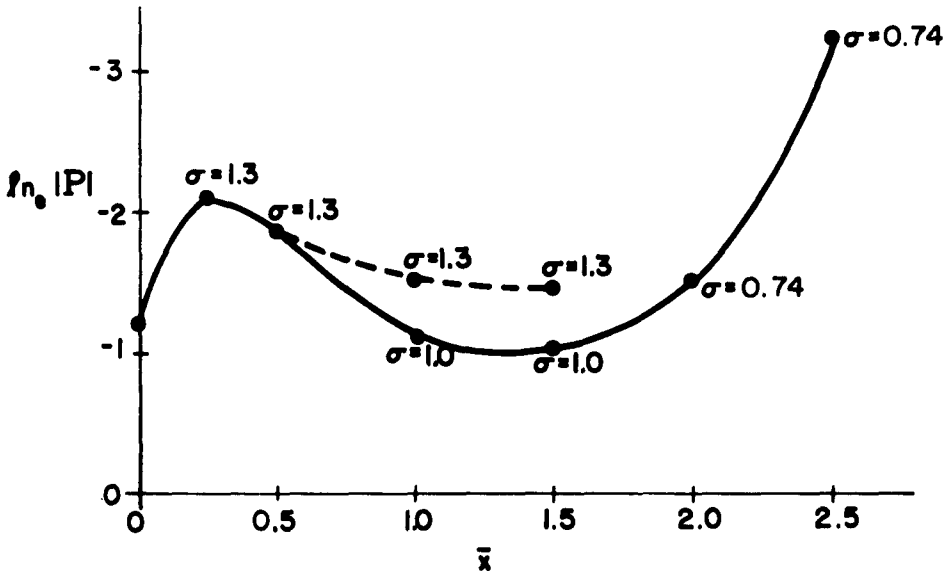

Fig. 5— Magnitude reflection factor illustrating sensitivity to σ ($f = 2 \times 10^7$)

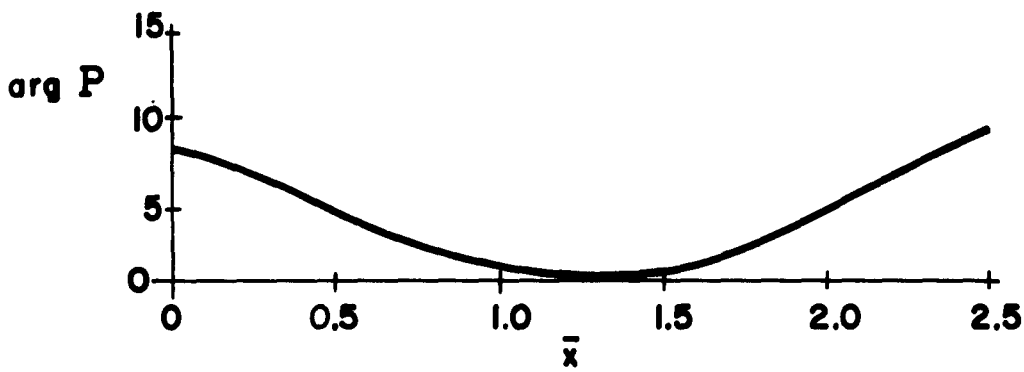

Fig. 6 — Phase of reflection factor, arg P, ($f = 2 \times 10^7$)

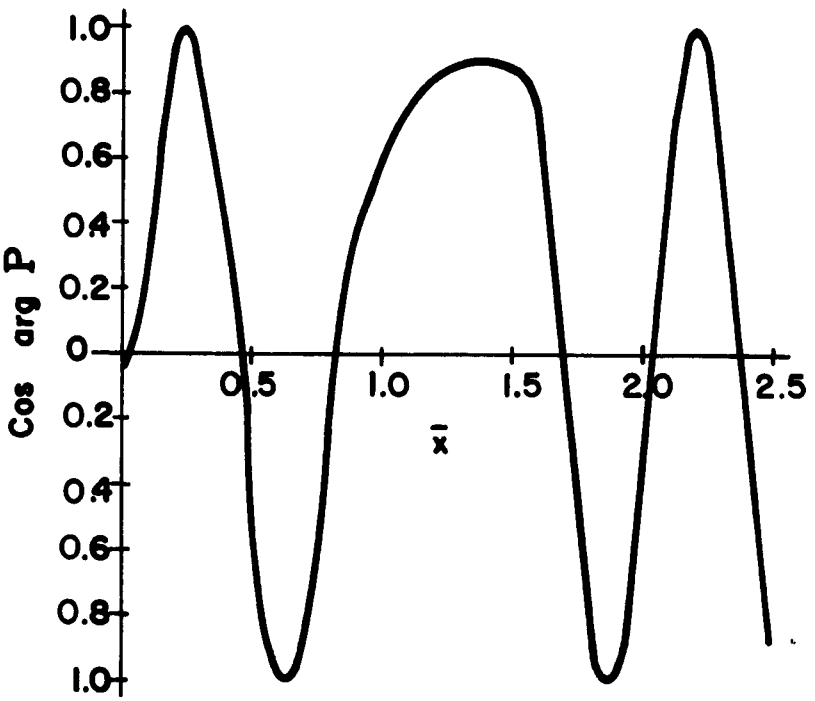

Fig. 7— Cos arg P $(f = 2 \times 10^7)$

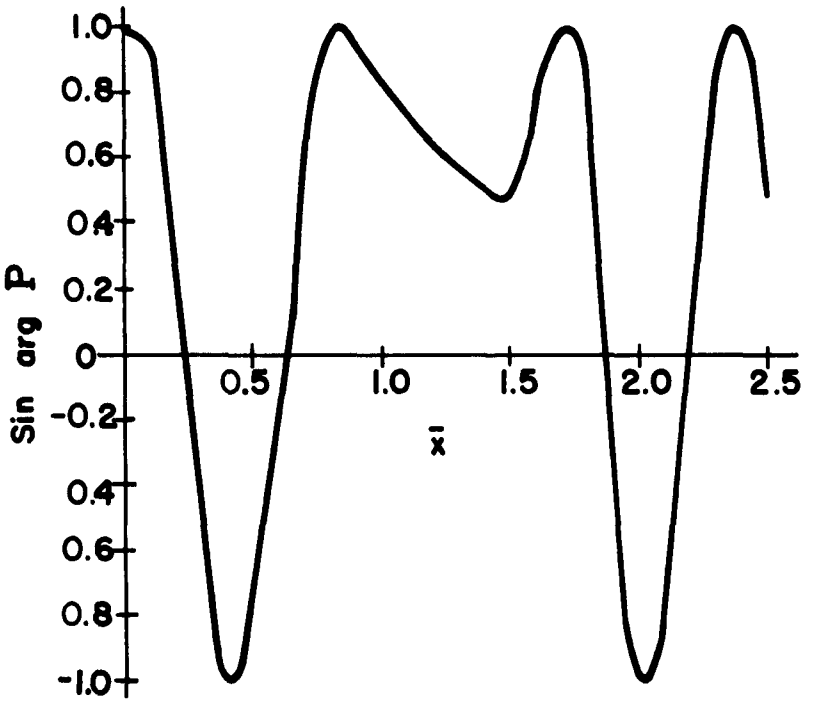

Fig. 8 — Sin arg P $(f = 2 \times 10^7)$

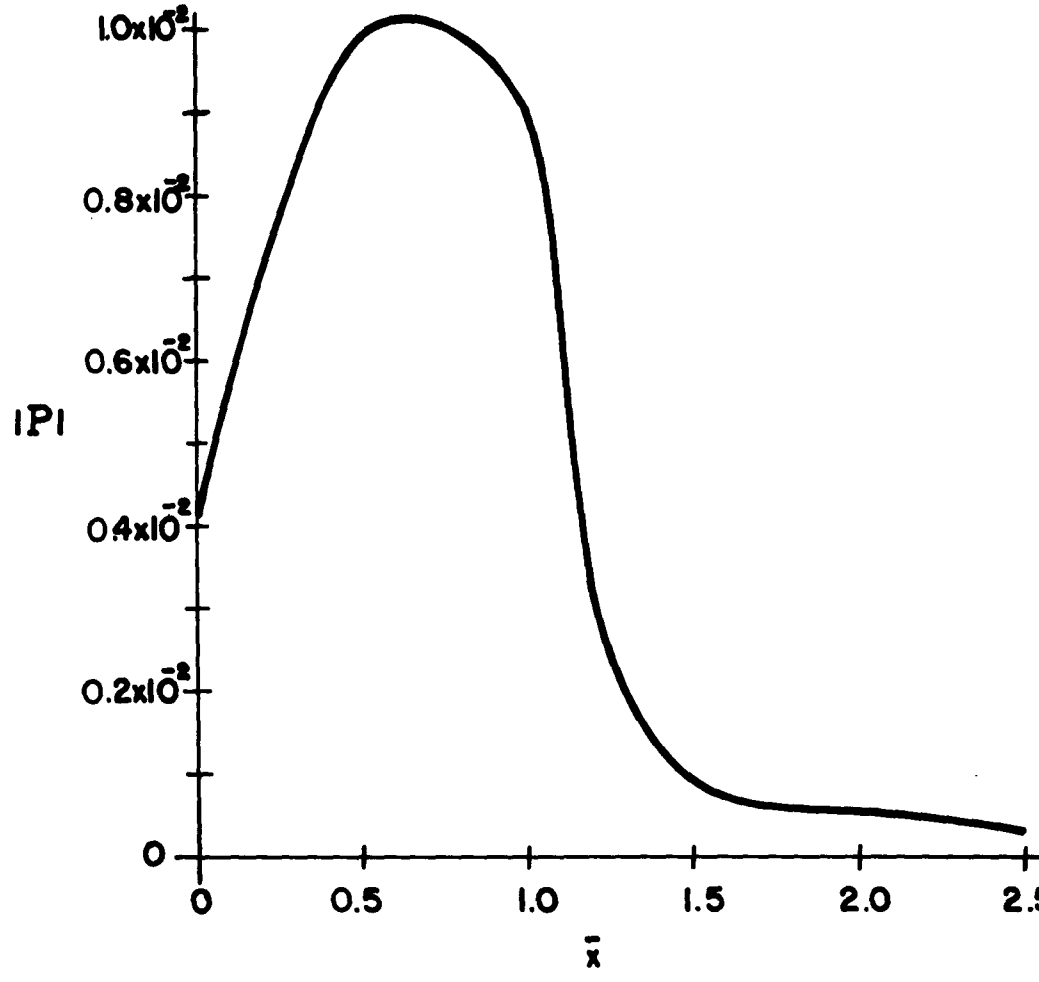

Fig. 9 — Magnitude reflection factor, $|P|$ ($f = 10^8$)

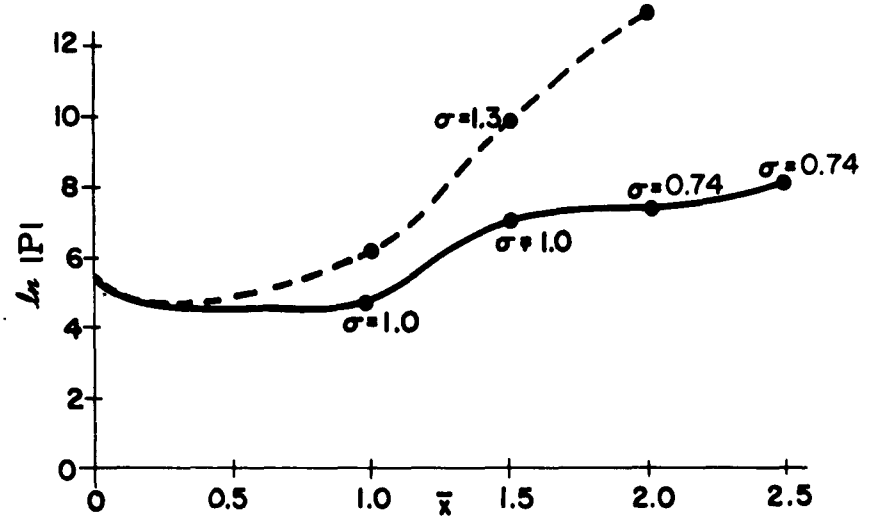

Fig. 10—Magnitude reflection factor illustrating sensitivity to σ ($f = 2 \times 10^8$)

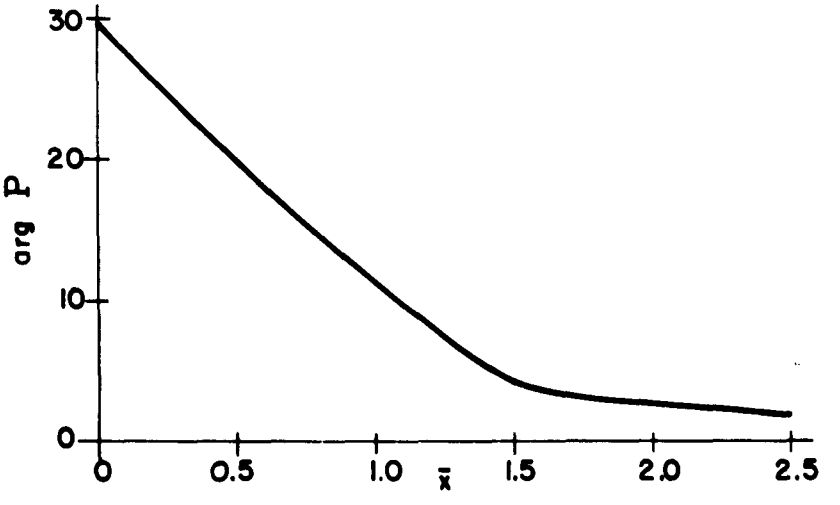

Fig. 11 — Phase of reflection factor, arg P ($f = 10^8$)

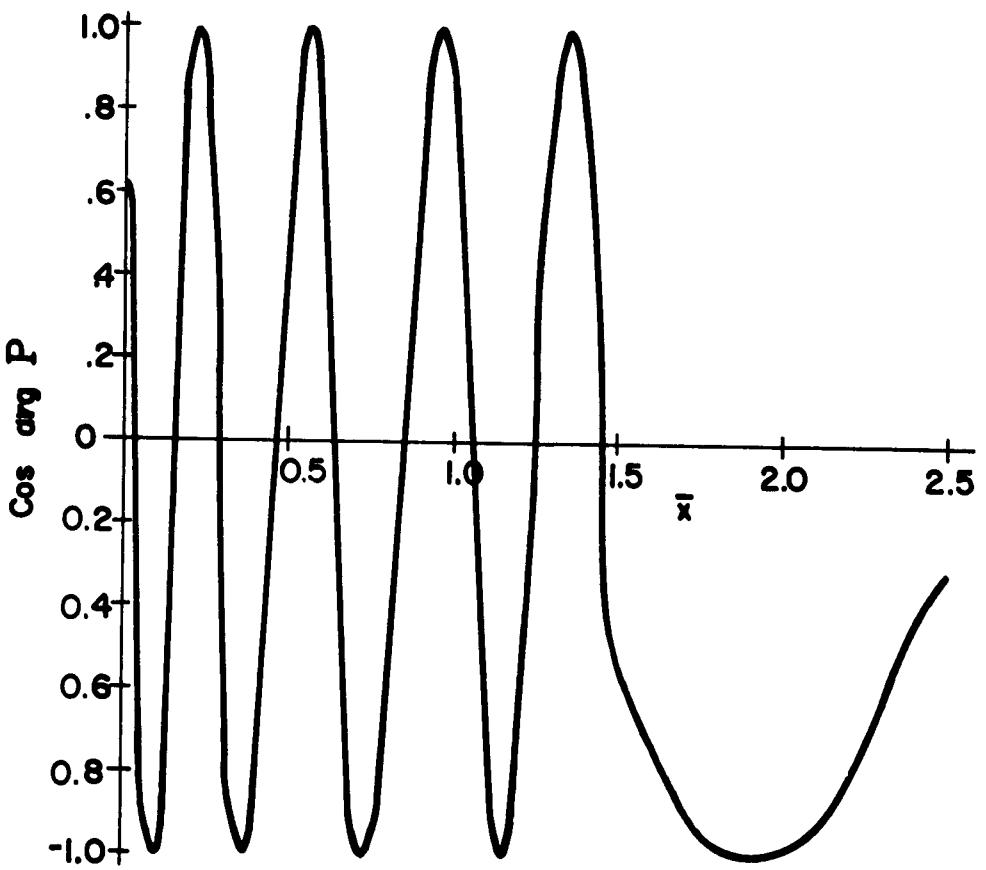

Fig. 12— Cos arg P $(f = 10^8)$

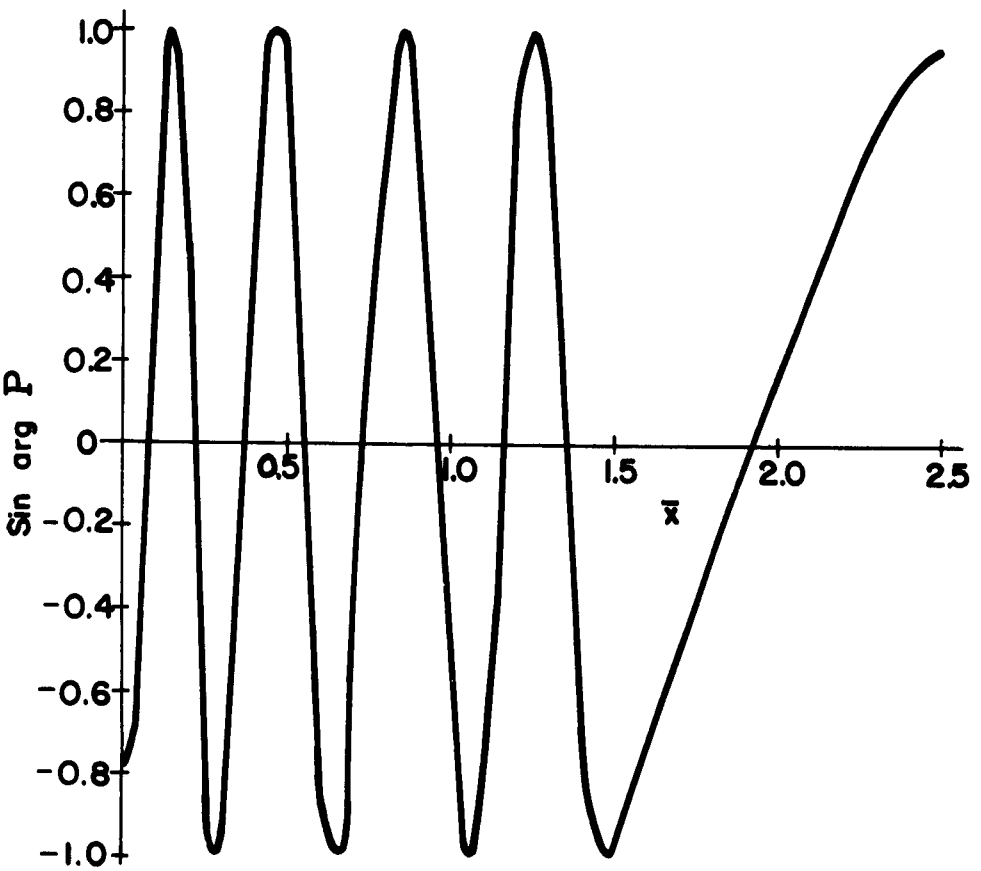

Fig. 13— Sin arg P $(f = 10^8)$

where $|I|^2 = \left| \int_0^{\bar{x}_m} |P| \exp(\arg P)\, d\bar{x} \right|^2$ and lengths are in centimeters.

For sphere-cylinders, $C_D \sim 0.9$ and $4\, C_D^2/\pi \sim 1$. Thus, for r_o in centimeters

$$\sigma \sim 220\, r_o^4\, s(ka)\, |I|^2 \text{ cm}^2$$

The results of the integrations and the corresponding cross sections for $r_o = 30$ cm are given below:

f	2×10^7 cps	10^8 cps
$\|I\|^2$	0.09	0.01
σ	600 m^2	320 m^2

To these σ values should be added the return of the trail region between the nose cone and the beginning of the expansion region $x = x_\infty$, and the return from the nose cone and surrounding plasma itself. The return from the trail for $x < x_\infty$ could, if desired, be computed in the same manner using the N_e values numerically obtained by Feldman.[1] However both these contributions will be negligible compared to the above σ values. Scattering from the nose cone itself will yield a $\sigma < 0.5$ m^2 while the trail region for $x < x_\infty$ is only about 10 r_o in length according to Ref. 2. Thus it too can have only a negligible effect on σ.

The trail length as measured to the position where N_e falls to $N_e \sim 10^8/cm^3$ is of the order of 3000 m, while the radius within which $N_e > 10^8/cm^3$ exceeds $2r_o$. Thus, as pne would expect considering the low reflectivity, the corresponding geometric cross section of the trail viewed broadside exceeds its radar cross section.

V. BASIC ELECTROMAGNETIC PROBLEM

In this Memorandum, the procedures used to estimate radar return from a re-entry wake form a patchwork set of approximations. To be sure, it is hoped they can yield computed results that agree with experimental observation. In this section we will discuss the problems involved in obtaining solutions that are more realistic from the electromagnetic aspect. Improvement of the wake-parameter computations and theory is not discussed.

We shall assume (for the most part) that the wake is composed of a cylindrically symmetric distribution of N_e and ν. This would, in many cases, rule out consideration of wakes behind vehicles that are following rapidly turning orbits or are unstable in flight. It also rules out turbulent wakes if the scale of turbulence is not small compared to the local radar wavelength in the wake. Turbulence of a scale that is small compared with the electromagnetic waves also presents two effects, the magnitude of which should be studied when enough data on the details of the turbulence become available. The first effect is that the turbulence will present to the electromagnetic waves a somewhat random array of small inhomogeneities in index of refraction. The Rayleigh scattering from these could probably be handled by methods such as those presented by Landau and Lifschitz.[27] The second effect of turbulence in an ionized medium is to produce a nonuniform distribution of current whirls. These will yield an effective magnetization current $\vec{J}_m$ and associated magnetization $\bar{M}$ through $\bar{J} = \text{curl } \bar{M}$. Then $\bar{B} = \mu_o (\bar{H} + \bar{M}) = \mu H$, where now $\mu \neq \mu_o$ as was previously assumed in the text. The additional difficulties presented to the electromagnetic problem by a variable permeability are discussed below.

The electromagnetic problem is to find a solution of Maxwell's equations which, far from the wake, behaves like the sum of a plane wave incident on the wake and a scattered field. Alternatively, we would look for the solution corresponding to an infinitesimal dipole source at a finite minimum distance from the cylinder (Green's function).

Let us consider the governing Maxwell's curl equations assuming $e^{-i\omega t}$ time-dependence.

$$\text{curl } \bar{E} = i\omega\bar{B} \tag{27}$$

$$\text{curl } \frac{\bar{B}}{\mu} = \frac{k^2n^2}{i\omega\mu_o}\ \bar{E} \tag{28}$$

These equations differ from the form of Eq. (11) in that μ is not taken to be the permeability μ_o of free space everywhere. We leave $\mu \neq \mu_o$ fo. the moment to bring out clearly the role a varying permeability plays in interlocking the equations. By the vector identity

$$\text{curl } a\,\bar{F} = \text{grad } a \times \bar{F} + a \text{ curl } \bar{F}$$

Eq. (28) may be rewritten as

$$\text{curl } \bar{B} = \frac{k^2n^2\mu}{i\omega\mu_o}\ \bar{E} + \frac{1}{\mu}\,\text{grad } \mu \times \bar{B}\ . \tag{29}$$

Taking the curl of Eq. (27) and substituting Eq. (29) yields the results

$$\text{curl curl } \bar{E} - k^2n^2\ \frac{\mu}{\mu_o}\,\bar{E} = \frac{i\omega}{\mu}\,\text{grad }\ \mu \times \bar{B} \tag{30}$$

When μ is constant the last term vanishes and an equation involving $\bar{E}$ alone is obtained.

In all ionospheric work it is assumed that $\mu = \mu_o$, and the resulting homogeneous equation is used. For example, the Epstein-layer analysis used in Section III is based on Eq. (30) with $\mu = \mu_o$. This is also assumed by DeRidder and Edelberg in Ref. 17. Through Eq. (33), let us now set $\mu = \mu_o$. Furthermore, when n^2 varies with only one coordinate so that iso-n^2 surfaces are planes, rectangular Cartesian coordinates are best adopted. There is then the added bonus that the x_i $(i = 1,2,3)$ component of curl curl $\bar{E}$ involves only the x_i component of $\bar{E}$. The plasma is electrically neutral in a macroscopic

sense so that div $\bar{E} = 0$ and

$$\text{curl curl } \bar{E} = \text{grad div } \bar{E} - \nabla^2 \bar{E} = -\nabla^2 \bar{E}$$

where for a rectangular coordinate system $\nabla^2 \bar{E}$ represents the operator

$$\frac{\partial^2}{\partial x^2} + \frac{\partial^2}{\partial y^2} + \frac{\partial^2}{\partial z^2}$$

Equation 30 becomes

$$\left(\frac{\partial^2}{\partial x^2} + \frac{\partial^2}{\partial y^2} + \frac{\partial^2}{\partial z^2} \right) \bar{E} + k^2 n^2 \bar{E} = 0 \qquad (31)$$

and this holds for each component of E separately. The equation for $E = E_y$ and n dependent on x only was used to derive the reflectivity formulas of Section III.

For cylindrical coordinates, only the z-component of curl curl $\bar{E}$ can be written out in a form containing only one component of E. Thus with

$$\nabla^2_{\text{cyl}} \psi = \frac{\partial^2 \psi}{\partial r^2} + \frac{1}{r} \frac{\partial \psi}{\partial r} + \frac{1}{r^2} \frac{\partial^2 \psi}{\partial \theta^2} + \frac{\partial^2 \psi}{\partial z^2} \qquad (32)$$

we have, for the z-component of the homogeneous form of Eq. (30)

$$\nabla^2_{\text{cyl}} E_z + n^2 k^2 E_z = -\frac{\partial}{\partial z} \text{ div } \bar{E} = 0$$

The other two components of Eq. (30) mix E_r, E_θ, and E_z, so that a separate equation cannot be obtained for E_θ or E_r alone. The right-hand side is zero, since div $\bar{E} = 0$.

Before pursuing this line further, let us first observe how even this decoupling is only one way since the assumption of spatially varying conductivity or effective dielectric constant which led to

a variable index of refraction n does not permit an equation in $\bar{B}$ alone to be written. Taking the curl of Eq. (29) yields

$$\text{curl curl } \bar{B} - \frac{1}{\mu^2} \text{ grad } \mu \times (\text{grad } \mu \times \bar{B}) - \frac{1}{\mu} \text{ curl } (\text{grad } \mu \times \bar{B})$$

$$-k^2 n^2 B = \frac{k^2}{i\omega} \text{ grad } (n^2) \times E = \frac{1}{n^2} \text{ grad } n^2 \times \text{curl } \frac{\bar{B}}{\mu} \quad (34)$$

Again terms drop out if μ is constant, which we once more assume.

If n^2 is a function of r only, further simplification occurs in the z-component equation, since grad n^2 is in the r direction and hence grad $n^2 \times \bar{E} = dn^2/dr \, E_\phi \hat{\phi}$. By Maxwell's equations

$$\dot{E}_\phi = \frac{i\omega}{k^2 n^2 \omega_o} (\text{curl } B)_\phi$$

The result is

$$\nabla^2_{cyl} H_z + k^2 n^2 H_z = - \frac{1}{n^2} \frac{dn^2}{dr} \left(\frac{\partial H_r}{\partial z} - \frac{\partial H_z}{\partial r} \right) \quad (35)$$

Finally, if only z-independent fields are permitted such as would occur at broadside incidence for radar scattering from an infinite circular cylinder, then $\partial H_r/\partial z = 0$ and a separated equation for H_z results. Therefore, E_z and H_z alone can be used to solve boundary value problems of broadside scattering; and the field components E_θ, E_r, H_θ, and H_r may all be obtained by the simple differentiations of H_z and E_z indicated by Maxwell's equations.

The equations to solve for E_z or H_z are each of the form

$$\frac{\partial^2 u}{\partial r^2} + \frac{1}{r} f(r) \frac{\partial u}{\partial r} + \frac{1}{r^2} \frac{\partial^2 u}{\partial \theta^2} + k^2 n^2 u = 0 \quad (36)$$

where k = constant and n^2 depends only on r^2. For E_z, $f(r) \equiv 1$;

for H_z, $f(r) = (1 - \frac{r}{n^2}\frac{dn^2}{dr})$. The form of Eq. (36) permits separation of variables. Thus let

$$u = \left.\begin{matrix}\cos m\theta \\ \sin m\theta\end{matrix}\right\} R(r) \tag{37}$$

where

$$R'' + \frac{f(r)}{r} R' + (k^2 n^2 - \frac{m^2}{r^2}) R = 0 \tag{38}$$

Were n a constant, the equation with $f(r) = 1$ would be simply that of the cylinder functions $Z_m(knr)$. If $n^2 = a^2 - b^2/r^2$ with a and b constants, we have as solutions cylinder functions of nonintegral order

$$Z_\nu (akr)$$

where

$$\nu = \pm\sqrt{b^2 k^2 + m^2}$$

In general as long as $\lim_{r \to 0} \frac{rf(r)}{r} = B_1$ and $\lim_{r \to 0} r^2(k^2 n^2 - \frac{m^2}{r^2}) = B_2$, where B_1 and B_2 are bounded, solutions may be obtained by classical methods as power series in r or power series in r plus logarithmically singular terms (the Bessel and Neumann cylinder functions in the above examples).

We can solve the electromagnetic problem for broadside incidence in a straightforward conventional way if we assume n = constant for $r > a$. Then the conventional expansion of a plane wave in Bessel functions $J_m(knr)$ can be used to express the incident wave. The reflected wave is then expressed as a superposition of Hankel functions with unknown coefficients to be determined. Using the requirement of continuity in E_z or H_z, these solutions can be matched to an expansion of the field for $r < a$ in terms of those nonsingular solutions of Eq. (38) which correspond to the chosen functional form of $n^2(r)$.

This is exactly the procedure employed in the extensive digital computations by DeRidder and Edelberg in Ref. 17, using several different functional forms and a wide range of parameter values.

To find the radar return from a nonuniform wake, one could use the results of such computations in an approximate way similar to that in which we used the Epstein reflectivity P and σ_c. For near-broadside incidence the results should in fact be better if the cylinder returns are available for the appropriate parameters. As is clear from the above, the results of Ref. 7 are based entirely on assuming broadside incidence. It can yield no results for off-broadside incidence, whereas the otherwise less-applicable Epstein reflectivity is not so limited, the effect of angle of incidence being expressed by the factor C occurring in the arguments of the gamma functions in Eq. (22). Likewise, the off-broadside solution for perfectly reflecting cylinders is available in Ref. 19. Thus the approximate methods used in this Memorandum can give off-broadside results, although their accuracy will degenerate as the aspect angle increases. Without successfully tackling the more general equations given above in this section, the accuracy or lack of accuracy of the approximate approach cannot really be gauged.

REFERENCES

1. Feldman, Saul, "Trails of Axi-Symmetric Hypersonic Blunt Bodies Flying Through the Atmosphere," J. Aero. Sci., Vol. 28, June 1961, pp. 433-448.

2. Lykoudis, P. S., Theory of Ionized Trails for Bodies at Hypersonic Speeds, The RAND Corporation, RM-2682, May 1961.

3. Shkarofsky, I. P., M. P. Bachynski, and T. W. Johnston, "Collision Frequency Associated with High Temperature Air and Scattering Cross-Sections of the Constituents," Research Report No. (7-801,5) RCA Victor Company, Ltd., Montreal, Canada, March 1960.

4. Feldman, Saul, "Numerical Comparison Between Exact and Approximate Theories of Hypersonic Inviscid Flow Plast Slender Blunt-Nosed Bodies," ARS Journal, Vol. 30, May 1960, pp. 463-468.

5. Gilmore, F. R., Equilibrium Composition and Thermodynamic Properties of Air to 24,000°K, The RAND Corporation, RM-1543, August 1955, (plus unpublished graphs).

6. Logan, J. G., and C. E. Treanor, "Polytropic Exponents for Air at High Temperatures," J. Aero. Sci., Vol. 24, June 1957, pp. 467-468.

7. Feldman, Saul, "Hypersonic Gas Dynamic Charts for Equilibrium Air," AVCO, Research Laboratory Report No. 40, January 1957.

8. Budden, K. G., Radio Waves in the Ionosphere, Cambridge, 1961.

9. Denisse, J. F., and J. L. Delcroix, "Theorie des Ondes Dans les Plasmas," Dunod, Paris, 1961.

10. Rawer, Karl, "Elektrische Wellen in einen geschichtenten Medium," Ann. der Phys., Vol. 35, July 1939, pp. 385-416.

11. Albini, F. A., and R. G. Jahn, "Reflection and Transmission of Electromagnetic Waves at Electron Density Gradients," Report TN3, Guggenheim, Jet Propulsion Center, California Institute of Technology, Pasadena, California, October 1960.

12. Albini, F. A., and R. G. Jahn, "Reflection and Transmission of Electromagnetic Waves at Electron Density Gradients," J. Appl. Phys., Vol. 32, January 1961, pp. 75-82.

13. Schelkunoff, S. A., "Remarks Concerning Wave Propagation in Stratified Media," in The Theory of Electromagnetic Waves, Interscience, New York, 1961.

14. Walther, Klaus, "Reflection Factor of Gradual-Transition Absorbers for EM and Acoustic Waves," IRE Trans. on Antennas and Prop. AP 8, November 1960, pp. 608-621.

15. Barrar, R. E., and R. M. Redheffer, "On Nonuniform Dielectric Media," IRE Trans. on Antennas and Prop., AP 3, July 1955, pp. 101-108.

16. Bellman, Richard, and Robert Kalaba, "On the Principle of Invariant Imbedding and Propagation through Inhomogeneous Media," Proc. Nat. Acad. Sci., Vo. 42, July 1956, pp. 629-632.

17. DeRidder, C. M., and S. Edelberg, "Scattering from Plasma Cylinders with Radial Variations in Electron Density," Lincoln Laboratory, MIT (preprint).

18. Brysk, H., "The Radar Cross-Section of a Semi-Infinite Body," Canadian Phys., Vo. 38, January 1960, pp. 48-56.

19. Mentzer, J. R., Scattering and Diffraction of Radio Waves, Pergamon Press, New York, 1955.

20. Peters, L., Jr., and W. G. Swarner, "Coherent Scattering of a Metallic Body in the Presence of an Ionized Shell," Scientific Report No. 2, Contract AF 19(604)-7270, Antenna Lab., Dept. of Elect. Engr., Ohio State University Research Foundation, March 1961.

21. Alred, R. V., "Scattering of Electromagnetic Waves by Metallic Spheres Covered with Absorbing Materials," Rpt. XRE-4/47/5, Admirality Signal Establishment, Witley, Surrey, England, December 1947.

22. Neugebauer, H. E. J., "Extension of Babinet's Principle to Absorbing and Transparent Materials, and Approximate Theory of Backscattering by Plane, Absorbing Disks," J. Appl. Phys., Vol. 28, March 1957, pp. 302-307.

23. Dolph, C. L., and H. Weil, "Enhancement of Radar Cross-Sections of Warheads and Satellites by the Plasma Sheath," in Electromagnetic Effects of Reentry, Pergamon Press, New York, 1961; reprinted in Planetary and Space Sci., Vol. 6, June 1961.

24. Brysk, H., "Electromagnetic Scattering by Low-Density Meteor Trails," Geophys. Res., Vol. 63, December 1958, pp. 693-716.

25. Brysk, H., "Electromagnetic Scattering by High Density Meteor Trails," IRE Trans. on Antennas and Propagation, AP 7, Special Supplement, Symposium on Electromagnetic Theory, December 1959, pp. S 330-S 336.

26. Tables of the Gamma Function for Complex Arguments, National Bureau of Standards, Applied Mathematics Series, 34, August 1954.

27. Landau, L. D., and E. M. Lifshitz, Electrodynamics of Continuous Media, English translation by J. B. Sykes and J. S. Bell, Addison-Wesley, 1960.